Statistical properties of fractal dendrites and anisotropic diffusion-limited aggregates

Y. Couder
Laboratoire de Physique Statistique, 24 rue Lhomond, 75231 Paris CEDEX 05, France

F. Argoul* and A. Arnéodo*
Department of Physics and the Center for Nonlinear Dynamics, University of Texas, Austin, Texas 78712

J. Maurer and M. Rabaud
Laboratoire de Physique Statistique, 24 rue Lhomond, 75231 Paris CEDEX 05, France
(Received 8 December 1989)

Crystalline dendrites, growing in a two-dimensional diffusion field at small Péclet numbers, are investigated. It is shown that, far from the tip, the distribution in size of the side branches gives them a fractal structure of dimension $d_f \approx 1.58 \pm 0.03$. In spite of the fluctuations, their overall area is the same as the underlying stable parabola observed at the tip. Similarly, anisotropic diffusion-limited aggregation patterns grown in a strip have a mean occupancy profile with a parabolic tip and a selection mechanism similar to that of stable anomalous Saffman-Taylor fingers.

Diffusion-controlled pattern-forming systems have been recent centers of interest.[1] Among them, dendritic crystal growth, viscous fingering, and diffusion-limited aggregation (DLA) have received the most attention. The fields in which the two latter patterns grow are Laplacian, while the former is a finite-range diffusive field. Experimental and theoretical efforts have been focused in two directions. On the one hand, the shape and selection mechanism of nonlinear *stable curved fronts* were investigated and analytical solutions were found. Notable examples are the parabolic needle crystal[1,2] and the Saffman-Taylor (ST) fingers in linear[1,3] and sector-shaped channels.[4] On the other hand, the very unstable patterns have been mainly considered from the point of view of their *fractal* structure.[1,5,6]

Roughly two different types of pattern morphologies are observed corresponding to isotropic and anisotropic growths. The aim of the present work is to study the structure of complex anisotropic patterns obtained in the three experiments listed above and to compare them to the stable solutions.[7] Anisotropic growths are characterized by the existence of preferential directions of growth. The term must be used with care as the anisotropy of growth of the pattern is not necessarily due to general microscopic anisotropy of the physical properties of the system; local effects can generate preferential directions of growth.[8]

The rough growth of monocrystals in an undercooled solution gives rise to the characteristic crystalline dendrites. These grow along the main axis of the crystal and have a parabolic tip. Their sides destabilize into lateral branches which compete and, far from the tip, form a complex pattern. The anisotropy of the growth is due to the anisotropy of the surface tension of the crystalline structure. Experimental[1,9,10] and theoretical efforts[1] have resulted in the understanding of the selection mechanism of the parabola. The characteristic length scale l_{MS} of the instability of a planar crystallization front growing at velocity V is given by the linear analysis of Mullins and Sekerka,[1(a)] $l_{MS} \propto (d_0 D/V)^{0.5}$, where D is a diffusion constant and d_0 a capillary length. The radius of curvature ρ of parabolic dendrites is proportional to l_{MS} (so that $\rho^2 V = \text{const}$); the proportionality coefficient is a decreasing function of ϵ, the surface tension anisotropy.[1]

Our first aim here is to study the general structure of an experimentally obtained complex dendrite, from the point of view of its fractal structure and of its relation to the analytical parabola. We will limit ourselves to the situation where the impurity diffusion field has a length scale ($l_D = D/V$), large when compared to the observed region of the dendrite. The screening-off between different branches is then the same as in a Laplacian field. However, l_D remains small as compared to the distance to the lateral walls of the cell so that the medium can be considered infinite.

We grew ammonium bromide crystals in conditions similar to those described in Ref. 10, but from a solution with a different concentration. As the thermal diffusivity is three orders of magnitude larger than the mass diffusivity, the system is limited by mass diffusion for which $D = 2 \times 10^{-9}$ m^2/s and we work at Péclet numbers $P_e \sim 10^{-3}$. In the following, the indices 1 and 2 will refer respectively to two dendrites, grown at velocity $V_1 = 0.6$ μm/s and $V_2 = 2.6$ μm/s, on which extensive measurements were done. The impurity diffusion lengths were $l_{D_1} = 3.3$ mm and $l_{D_2} = 0.78$ mm. The cell thickness $E = 30$ μm was small compared to l_D, so that the diffusion field could be considered as two dimensional. Near the tip the situation remained three dimensional because the tip radius $\rho < e$. One single, well-oriented germ (two [100] axes in the cell's plane) initiated the growth

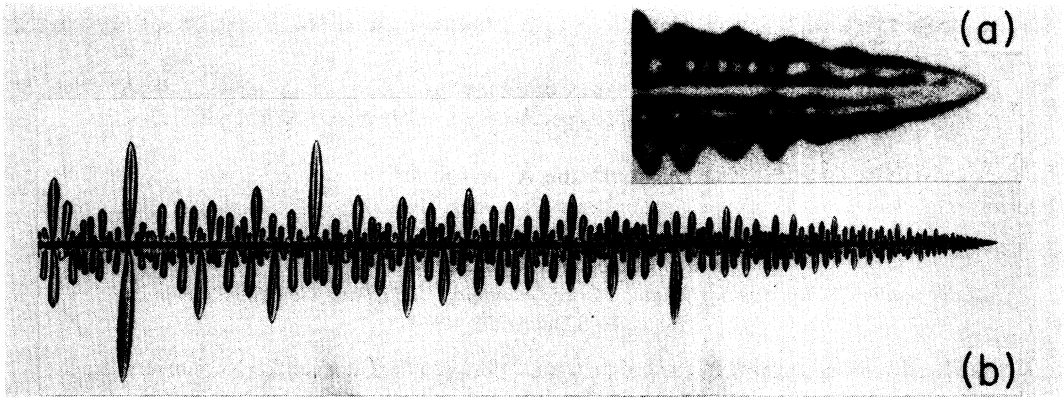

FIG. 1. (a) Tip region (of length 20ρ) of a dendrite showing its stable parabolic tip and the initial destabilization. (b) Photograph of a region of length 500ρ of the same dendrite (here $\rho=2.5$ μm).

and we waited long enough to get a sufficiently developed dendrite far away (more than a centimeter) from the boundaries and from the other main arms grown from the germ.[11] In the following the origin is at the tip, Ox is along, and Oy across the dendrite. By means of a 35-mm camera and a videocamera, we first recorded the detailed shape of the dendrite tip [Fig. 1(a)]. In this region we determined by image processing[10] the parabola which was the best fit to the stable part of the profile extending over a length $\Delta x \sim 4\rho$. We found $\rho_1=3.8\pm0.1$ μm and $\rho_2=1.7\pm0.1$ μm, respectively. The corresponding values $\rho_1^2 V_1=7.4\pm0.2$ μm^3/s and $\rho_2^2 V_2=7.5\pm0.2$ μm^3/s are in good agreement with each other. We simultaneously recorded the unstable dendrite in a large region behind the tip [Fig. 1(b)]. The hierarchy of sizes of the side branches makes the dendrites fractal objects even though, due to anisotropy, they are compact along their axis.[12] We image processed a part of the dendrite far from the tip, analyzed it by the box-counting method, and found a fractal dimension $d_f=1.58\pm0.03$ in agreement with the dimension ($d_f=1.57$) found numerically for fourfold anisotropic DLA.[13,14] Finally, we wanted to do statistical measurements on the whole structure. We chose, for each value of the distance x_0 to the tip, to measure the dendrite area $S(x_0)$ from the tip to x_0. Figure 2 shows a logarithmic plot of $S(x_0)$ as a function of x_0. Over three orders of magnitude of length scales $S(x_0)$ vary as $(x_0)^{1.5}$, as would have been expected if the dendrites had had a smooth parabolic shape. Furthermore, in the range $10\rho<x_0<1000\rho$, the coefficient of proportionality gives $\rho_1=3.7\pm0.1$ μm and $\rho_2=1.7\pm0.1$ μm, respectively, the same values as for the stable tip. The mean parabolic shape occupied by the unstable dendrite is thus the parabola of the stable tip. A parabolic dependence of the unstable dendrite could be expected from Ivantsov's simple qualitative argument:[1,2] the tip of the dendrite moves at constant velocity so that its position is proportional to the time t; the growth of the lateral sides results from a diffusive process and their position moves as $t^{0.5}$. However, there is more to our result. We find that *the selected solution for the mean of the fractal object and for the compact one are the same* (here a parabola with the same ρ).

To find this smooth average profile we would also measure a rate of mean occupancy $r(x,y)$ on many runs of the same experiment. The stable parabola is then uncovered by determining for each x the value y_m of y such that

$$y_m(x)=\frac{1}{r_{\max}}\int_0^{\infty} r(x,y)\,dy \ , \tag{1}$$

where $r_{\max}$ is the maximum value of $r(x,y)$ along the growth's axis Ox. This result can be compared[15] to that obtained in a previous work[7] in which we had shown that isotropic fractal ST fingers and DLA clusters grown in

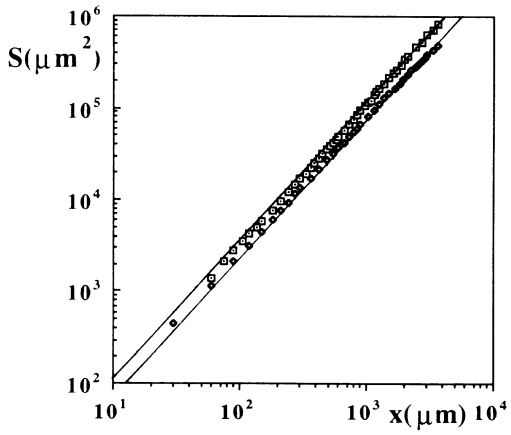

FIG. 2. Logarithmic plot of the surface $S(x_0)$ of dendritic patterns as a function of the distance x_0 to the tip. □, $S_1(x_0)$; ◇, $S_2(x_0)$. The solid lines correspond to the surfaces of compact parabolic dendrites with the same radius of curvature $\rho_1=3.7$ μm and $\rho_2=1.7$ μm as the fractal dendrites 1 and 2, respectively.

linear and sector-shaped channels[4] retained statistically the structure and selection of the stable solution; in each type of experiment, when a large number of runs was performed, the region of the cell with large mean occupancy had the width and shape of the stable ST finger in this geometry.

We wish now to extend these results to unstable patterns in ST fingering and DLA when a preferential direction of growth exists. The viscous fingering instability for a front moving at velocity V is characterized by its capillary length scale $l_c \propto (V)^{-0.5}$. Viscous fingering usually creates isotropic patterns. Several global[16] and local[8,17–19] means have been used to create preferential directions of growth. These are well observed in the circular configuration but their selective effect can be measured quantitatively in the linear cells[17(b),17(c)] in which they result into narrow ST fingers with a parabolic tip scaled on l_c. As for dendrites, the relation $\rho^2 V = \text{const}$ is satisfied and the finger exhibits dendritic side branches. In our experiment we used linear cells, giving one of their plates a periodic structure in two perpendicular directions[16] by stretching over it a thin nylon tulle cloth of thickness 0.2 mm. Typical unstable fingers are shown in Figs. 3(a) and 3(d) when the direction of the weaving is respectively along the cell axis or 45° away from it. The results are similar to those of anisotropic DLA. We will here limit ourselves to the presentation of the results for DLA aggregates; they have exact counterparts in unstable ST growth.

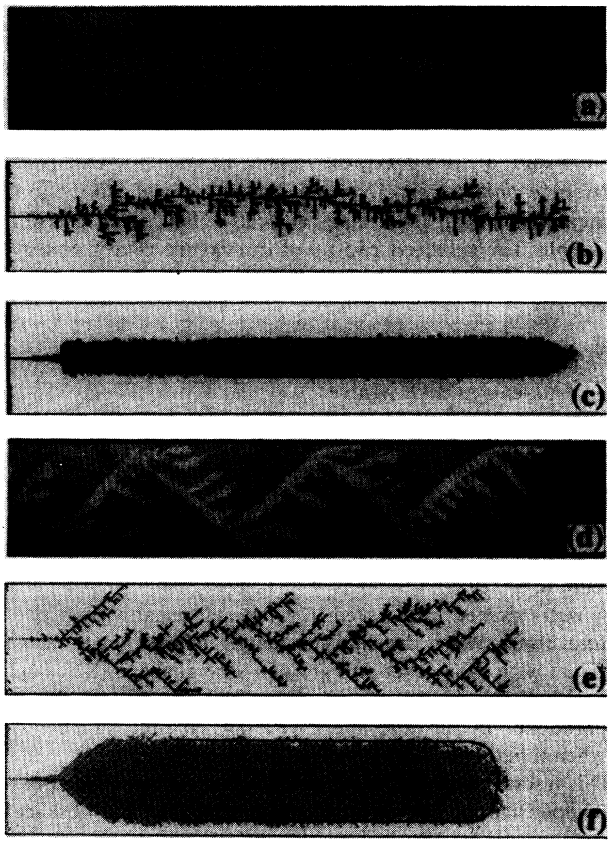

FIG. 3. Anisotropic patterns in linear cells. In both ST fingers and DLA clusters, patterns with strong or weak anisotropy differ by the stability of their tip. The pictures were chosen so as to show the two situations: (a) and (d) have strong anisotropy, (b) and (e) weak anisotropy. (a) Unstable ST finger in a cell ($W=10.5$ cm, $b=0.5$ mm) when an axis of easy growth is along the channel. (b) A noise-reduced (with $m=3$) DLA cluster of 2000 particles grown in a strip of width $W=64$, the lattice being parallel to the strip. (c) The points of the strip where the occupancy rate is larger than $R(y_m)$ are represented in gray. This repartition was obtained from the analysis of 250 aggregates of the type shown in (b). The continuous line is the shape of the ST analytical solution of width $\lambda=0.38$. (d) Unstable ST finger in the same cell as in (a) when both easy axes are 45° off the direction of the channel axis. (e) A $M=1600$ noise-reduced DLA aggregate (with $m=3$), the lattice being at 45° from the axis of the strip ($W=64\sqrt{2}$). (f) Points of the strip with occupancy $r>r(y_m)$ in the case of 250 aggregates of the type shown in (e); the solid line corresponds to the analytical ST solution of width $\lambda=0.77$.

A DLA front is instable at a scale given by the grid unit size l_u. No stable curved front is observed. From the point of view of isotropy, DLA corresponds to a specific situation. Previous results show that the system has microscopic anisotropy because of the sticking rule of the particles on the square lattice. But in the most usual case the anisotropy is hidden by the large noise of the random walk. If the noise of the system is reduced,[13] the resulting clusters do show preferential directions of growth along the lattice axes. The resulting effective anisotropy is controlled by a noise-reducing parameter, but is actually not known quantitatively. We computed DLA clusters in strip geometries,[7] introducing a noise-reducing procedure: each lattice site adjacent to the cluster has a counter and a random walker only sticks onto it when a number m of visits has been reached. The larger m, the larger the effective anisotropy of the medium. In a given strip, we grew N aggregates with the same total number M of particles. For instance, Fig. 3(b) shows one out of 250 aggregates of mass $M=2000$ grown in a channel of width $W=64$ when the lattice is oriented along the cell's axis. We then counted for each point of the grid how many times it had been occupied by a particle of an aggregate. This number, divided by N, gives $r(x,y)$, the mean occupancy of this point. All transverse occupancy profiles have a maximum value $r_{\max}$ on the axis of the strip and decrease to zero at the walls ($y=\pm W/2$). When the lattice is parallel to the cell's axis, the peak is narrow and there is a large region on each side where $r=0$. We determined the points y_m satisfying condition (1). This procedure appears more general than the cut at midheight[15] ($r_{\max}/2$) originally used for unstable ST fingers and DLA clusters grown in a strip.[7] Unlike the isotropic case, for a given m, the width of the region of large occupancy depends on the width of the cell. For instance for $m=3$ we find $\lambda=0.38\pm0.02$ for $W=64$, $\lambda=0.27\pm0.02$ for $W=128$, and $\lambda=0.21\pm0.02$ for $W=256$. Figure 3(c) shows all the points of a strip $W=64$ where r is larger than $r(y_m)$. The limit of this region is well fitted by the ST solution of corresponding λ. The radius of curvature at the tip can thus be deduced

from the analytical equation:[3,17(b)] $\rho=(\lambda^2 W)/\pi(1-\lambda)$. In the three strips investigated we found (in lattice units) $\rho_{64}=4.6\pm0.5$, $\rho_{128}=4.2\pm0.6$, and $\rho_{256}=4.6\pm0.8$, respectively, a constant value showing that, *for a given effective anisotropy, the width of large occupation is selected by its radius of curvature at the tip.* This is precisely the main characteristics of stable anomalous viscous fingers.[17(b)] Finally, experiments performed with different values of m show that the selected radius of curvature is a decreasing function of the noise-reducing parameter. We found $\rho=6.4\pm0.8$, 4.6 ± 0.5, 2.6 ± 0.2, and 1.8 ± 0.3, respectively, for $m=2$, 3, 4, and 5. (At large values of m the cutoff value induced by the grid mesh size is reached and the aggregate, like a dendrite, is compact at its tip.) Although there is no surface tension in this problem, this behavior is qualitatively similar to that induced by surface tension anisotropy in crystal growth and gives a quantitative support to the visual impression that an effective anisotropy could be defined related to m.

Finally, it is worth investigating the case where anisotropy is 45° off the cell axis.[20] In both ST fingering [Fig. 3(d)] and DLA [Fig. 3(e)], the pattern occupies a large portion of the cell. The limit of the region of large mean occupancy can be fitted by the ST solutions of relative width $\lambda>0.5$ [Fig. 3(f)], though the statistical noise is here important. Comparison of these mean profiles with a corresponding stable solution is not possible because when the anisotropy is this direction, no stable finger is observed.

Compact isotropic structures (ST fingers) and anisotropic ones (dendrites and anomalous ST fingers) obey different selection rules. The present paper and Ref. 7 show that both types of selections extend to unstable fractal patterns.[21] In the isotropic case, the mean solution is selected by the larger length scale of the system (the channel width). In the anisotropic case, it is selected by the radius of curvature at the tip of the mean profile. This radius ρ is proportional to the small scale (l_{MS}, l_c, or l_u). The proportionality coefficient is a decreasing function of an effective anisotropy. When it is large (dendrites and DLA at large m), ρ is of the order of l_{MS}, l_c, or l_u, and a stable region exists at the tip; the fractal structure only results from the growth away from the tip. When it is small, the noise-reduced DLA, the tip itself is unstable; the selected radius of curvature is not observed on a given realization, but it still exists as a statistical property.

We would like to acknowledge useful discussions with G. Grasseau and O. Maire.

---

*Permanent address: Centre de Recherche Paul Pascal, Avenue Schweitzer, 33600 Pessac, France.

[1]For reviews see (a) J. S. Langer, Rev. Mod. Phys. **52**, 1 (1980); (b) S. C. Huang and M. E. Glicksman, Acta Metall. **29**, 701 (1981); (c) D. Bensimon, L. P. Kadanoff, S. Liang, B. I. Shraiman, and Chao Tang, Rev. Mod. Phys. **58**, 977 (1986); (d) J. S. Langer, in *Chance and Matter,* edited by J. Souletie, J. Vanimenus, and R. Stora (North-Holland, Amsterdam, 1987); see also J. S. Langer, Science **243**, 1150 (1989); (e) D. A. Kessler, J. Koplik, and H. Levine, Adv. Phys. **37**, 255 (1988); (f) P. Pelcé, *Dynamics of Curved Fronts* (Academic, Orlando, 1988); (g) *Random Fluctuations and Pattern Growth,* edited by H. E. Stanley and N. Ostrowsky (Kluwer Academic, Dordrecht, 1988); (h) T. Vicsek, *Fractal Growth Phenomena* (World Scientific, Singapore, 1989), and references therein.

[2]G. P. Ivantsov, Dokl. Acad. Nauk SSSR **58**, 567 (1947).

[3]P. G. Saffman and G. I. Taylor, Proc. R. Soc. London, Ser. A **245**, 312 (1958).

[4]H. Thomé, M. Rabaud, V. Hakim, and Y. Couder, Phys. Fluids A **1**, 224 (1989).

[5]T. A. Witten and L. M. Sander, Phys. Rev. Lett. **47**, 1400 (1981); Phys. Rev. B **27**, 5686 (1983).

[6]S. N. Rauseo, P. D. Barnes, and J. V. Maher, Phys. Rev. A **35**, 1245 (1987); Y. Couder, Ref. 1(g), p. 75.

[7]A. Arnéodo, Y. Couder, G. Grasseau, V. Hakim, and M. Rabaud, Phys. Rev. Lett. **63**, 984 (1989).

[8]Effective anisotropic growth induced by local disturbances has been observed in the Saffman-Taylor problem—experimentally with a small bubble [Refs. 17(a) and 17(b)], a thread, or a groove [Refs. 17(b) and 17(c)]; numerically when the surface tension has a singular zero or infinite value at a point of the front [Ref. 17(c)]. Theoretically it was shown analytically that the selection of these solutions could be due to a positive or a negative cusp (Ref. 18) on the front or to a disturbance of the flow at a finite distance of the finger tip (Ref. 19).

[9]A. Dougherty and J. P. Gollub, Phys. Rev. A **38**, 3043 (1988).

[10]J. Maurer, P. Bouissou, B. Perrin, and P. Tabeling, Europhys. Lett. **6**, 67 (1989).

[11]A well-oriented initial seed in a flat cell usually gives rise to four arms. When the diffusion length is large, these arms interact with each other and grow in a petal shape (Ref. 14). It is only the front part of each arm which can be considered as parabolic. In our experiment we analyzed 2 mm of a dendrite when it had grown 1 cm away from the seed.

[12]This fractal character of the dendrites is directly related to the competitive interaction in a long-range field. The absence of this process leads to completely different patterns. If a dendrite is grown from an initial seed at high velocity (high Péclet number), it will form a diamond-shaped pattern because the different branches do not have interacting fields and all grow at the same velocity.

[13]J. Nittmann and H. E. Stanley, Nature **321**, 663 (1986); J. Kertèsz and T. Vicsek, J. Phys. A **19**, L257 (1986); P. Meakin, Phys. Rev. A **36**, 332 (1987); P. Meakin, J. Kertèsz, and T. Viczek, J. Phys. A **21**, 1271 (1988).

[14]J. P. Eckmann, P. Meakin, I. Procaccia, and R. Zeitak, Phys. Rev. A **39**, 3185 (1989).

[15]The occupancy rate $r(x,y)$ has different profiles for isotropic (Ref. 7) and anisotropic structures. In the former case we have checked that the values y_m given by relation (1) coincide exactly with those deduced from a cut at midheight ($r_{\max}/2$). In the latter case they differ. In the dendrites, for instance, $r_{\max}=1$ near the axis. Two transverse histograms at x_1 and x_2 only differ by their falloff at large y (small r) because only the large side branches keep growing. Relation (1) accounts for this evolution while a cut at midheight would not. Condition (1) thus applies to both the isotropic and anisotropic situations and is the most general procedure to obtain the mean profile.

[16]E. Ben-Jacob, R. Godbey, N. D. Goldenfeld J. Koplik, H. Levine, T. Mueller, and L. M. Sander, Phys. Rev. Lett. **55**, 1315 (1985).

[17](a) Y. Couder, O. Cardoso, D. Dupuy, P. Tavernier, and W. Thom, Europhys. Lett. **2**, 437 (1986); (b) M. Rabaud, Y. Couder, and N. Gérard, Phys. Rev. A **37**, 935 (1988); (c) G. Zocchi, B. E. Shaw, A. Libchaber, and L. P. Kadanoff, *ibid.* **36**, 1894 (1987).

[18]D. C. Hong and J. S. Langer, Phys. Rev. Lett. **56**, 2032 (1986); Phys. Rev. A **36**, 2325 (1987).

[19]R. Combescot and T. Dombre, Phys. Rev. A **39**, 3525 (1989); and H. Thomé, R. Combescot, and Y. Couder (unpublished).

[20]G. Li, D. Kessler, and L. M. Sander, Phys. Rev. A **34**, 3535 (1986).

[21]A similar result has been obtained in Ref. 14 for the petal-shaped envelope of s-fold anisotropic DLA in the dendritic limit of very large noise-reducing parameter m.

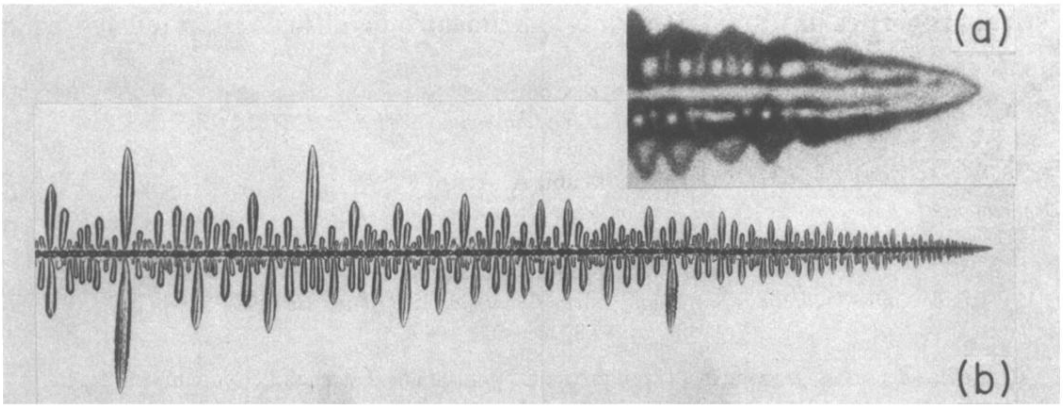

FIG. 1. (a) Tip region (of length 20ρ) of a dendrite showing its stable parabolic tip and the initial destabilization. (b) Photograph of a region of length 500ρ of the same dendrite (here $\rho = 2.5\ \mu$m).

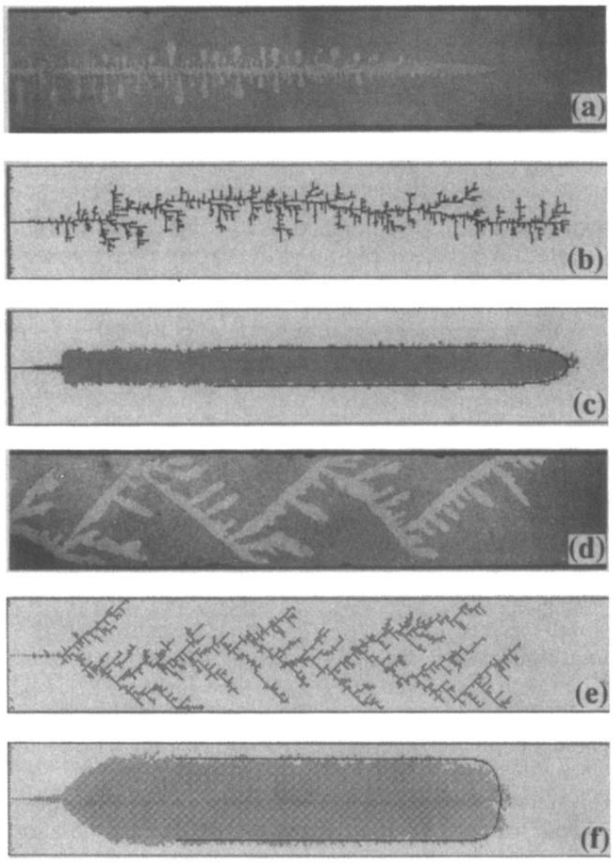

FIG. 3. Anisotropic patterns in linear cells. In both ST fingers and DLA clusters, patterns with strong or weak anisotropy differ by the stability of their tip. The pictures were chosen so as to show the two situations: (a) and (d) have strong anisotropy, (b) and (e) weak anisotropy. (a) Unstable ST finger in a cell ($W=10.5$ cm, $b=0.5$ mm) when an axis of easy growth is along the channel. (b) A noise-reduced (with $m=3$) DLA cluster of 2000 particles grown in a strip of width $W=64$, the lattice being parallel to the strip. (c) The points of the strip where the occupancy rate is larger than $R(y_m)$ are represented in gray. This repartition was obtained from the analysis of 250 aggregates of the type shown in (b). The continuous line is the shape of the ST analytical solution of width $\lambda=0.38$. (d) Unstable ST finger in the same cell as in (a) when both easy axes are 45° off the direction of the channel axis. (e) A $M=1600$ noise-reduced DLA aggregate (with $m=3$), the lattice being at 45° from the axis of the strip ($W=64\sqrt{2}$). (f) Points of the strip with occupancy $r>r(y_m)$ in the case of 250 aggregates of the type shown in (e); the solid line corresponds to the analytical ST solution of width $\lambda=0.77$.